Available online at www.sciencedirect.com
SCIENCE DIRECT
Fusion Engineering and Design 81 (2006) 873–877
Fusion Engineering and Design
www.elsevier.com/locate/fusengdes

IFMIF lithium loop activation and associated operator dose rates

W.E. Han *,[1], P.J. Karditsas [1]

Euratom/UKAEA Fusion Association, Culham Science Centre, Abingdon, Oxfordshire OX14 3DB, United Kingdom

Received 1 February 2005; received in revised form 9 August 2005; accepted 29 August 2005
Available online 27 December 2005

Abstract

An analysis has been made of the IFMIF lithium loop activation using the time-dependent, activation, transport and deposition code, TRACT (*TR*ansport of *ACT*ivation). Corresponding operator dose rates have also been derived using the neutron and photon transport Monte Carlo code MCNP-4C, enabling an assessment of operator exposure, both during IFMIF operation and for times up to 1 year after operation has halted. The dose rates were obtained for specific configurations of loop geometry. Where comparisons can be made, these results agree very well with those of an earlier preliminary investigation.

Keywords: IFMIF; Fusion; Lithium loop; Neutron activation; Corrosion products; Operator dose

1. Introduction

IFMIF operator doses could arise from activation of the liquid lithium (which is categorised as 'coolant' in the context of the modelling system employed) and any corrosion products deriving from wetted surfaces of the loop. Corrosion and coolant-carried corrosion products in the target area are activated by the deuteron beam and by the induced neutrons from the nuclear reactions. In this study, using the code TRACT [1], only the neutron activation is treated.

Following these calculations, resulting activation data are used to perform calculations of operator dose using the neutron and photon transport Monte Carlo code MCNP-4C.

2. Activation model: the code TRACT and data

2.1. The model

The code TRACT has been written from first principles in order to handle any gaseous or liquid coolant encountered in fusion devices and has the capability

* Corresponding author. Tel.: +44 1235 466390/528822; fax: +44 1235 466435.
E-mail address: winston.han@ukaea.org.uk (W.E. Han).
[1] Tel.: 44 1235 528822.

0920-3796/$ – see front matter © 2005 W.E. Han. Published by Elsevier B.V. All rights reserved.
doi:10.1016/j.fusengdes.2005.08.036

to treat an unrestricted number of stable and active species. TRACT allows for direct generation of active species in both the bulk wall material and in the coolant, and models the behaviour of the channel wall deposits as well as material carried in the coolant in the form of both solute and insoluble (crud) atoms/ions. This allows prediction of activity and its distribution throughout the loop for both *in-flux* and *out-of-flux* positions, possible occupational radiation exposure, the behaviour during normal operation, and the determination of the source term in hypothetical accidents that might involve coolant releases.

The code models the time-dependent behaviour of the coolant as it flows through the loop circuit and calculates the number density distribution of both active and non-active species, solving the time-dependent coupled coolant transport and bulk-solid diffusion mass transfer equations. Coolant soluble species production mechanisms include neutron activation, bulk-solid material corrosion product release and, in the case of crud deposits, release of these deposits by re-dissolution and erosion (not treated here). The rate of dissolution of deposited material is proportional to the deposited layer thickness and the concentration gradient between the surface (solubility) and the coolant.

Coolant species loss mechanisms include radioactive decay (active species), deposition onto surfaces and convective transport around the loop. Deposition is driven by a gradient between the bulk coolant and channel surface concentrations, but also depends on local flow conditions and the cooling channel surface area.

The release rate of corrosion products is assumed proportional to the amount of corroded material, and to the concentration gradient between the surface and the bulk fluid. Initially, there is no bulk fluid concentration, no deposit layer, and the rate of release of corroded material is expected to be high. As the soluble ion concentration in the coolant gradually builds up, conditions in some parts of the loop will be such that the local solubility concentration value is exceeded, leading to the formation of precipitate, i.e., "crud" particles. Once formed, precipitate will, on the average, continue to circulate in the system for some characteristic residence time, but any particles impacting the wall, and remaining there, will build up a deposit layer. The deposition rate varies along the loop, according to local mass transfer conditions.

2.2. Initial data

The Li coolant used in IFMIF is assumed to have the natural isotopic ratio, with no impurities. The backplate, piping and other loop components are assumed to be of SS316; the composition with impurities was taken from the SEAFP study [2].

Although ^{7}Be, which will be produced by the D-Li reactions, is not accounted for, it is intended that filtering will remove most, but not all, of this nuclide, leaving a residual ^{7}Be content of about 1 appb [3]. TRACT has the capability to include filtering, but this option was not used in this study.

A number of other parameters relevant to the IFMIF Li loop were obtained from the IFMIF Comprehensive Design Report (CDR) [4], and the loop geometry was obtained from information provided by EFDA CSU, Garching.

The value of the corrosion rate (kg/m^2 s) of stainless steel by lithium, used in this study, is given by:

$$G_{\mathrm{C}} = 1.433 \times 10^{-7}\, t^{-0.3} \tag{1}$$

where t is elapsed time since the start of IFMIF operation in seconds. The adopted rate reflects the specification given in the IFMIF CDR [4], which does not distinguish between *corrosion* and *dissolution*, but gives the 'corrosion/release' rate as 50 μm over 30 years. This value was taken as the corrosion rate for the purposes of the present study, although data in Ref. [5] reveal experimental values of SS316 corrosion in flowing lithium as high as 100 μm/year. However, the time exponent suggested by the latter reference is the one we have employed.

Solubility of SS316 in lithium dictates the local dissolution and crud-formation rates. The lithium-SS316 chemistry is not known and, in this study, it is assumed that the solubility of iron, the major constituent in SS316, controls the entire process. The remaining constituents are assumed to co-dissolve at a rate proportional to their fraction in the material. After fitting the relevant data for IFMIF conditions, given in Ref. [6] as a function of temperature, T, in Kelvin, the solubility, S (mol%), of iron in lithium can be expressed as

$$\log_{10} S = -2.485 - 247.1/T \tag{2}$$

It should be recalled that TRACT is modelling *flowing* lithium, and that the only region assumed to undergo

neutron irradiation is the target region. Thus any fluid element of lithium is subjected to irradiation only during passage across the deuteron beam, a very short time duration compared to the time for one circuit of the loop. The neutron spectrum, provided by FZK, Karlsruhe, in 211 energy groups up to 60 MeV, corresponding to IFMIF full operation conditions of 40 MeV at 250 mA, was averaged over the region of Li falling within the deuteron beam footprint. This spectrum was combined with cross section data with the aid of the neutron activation code, FISPACT, using the European Activation System, EASY-2004 [7], and the results were formatted for use as a TRACT input file. The 2004 version of EASY has new nuclear data libraries extended to 60 MeV neutron energy, to enable IFMIF modelling. Some cross sections in this first version of the high-energy library have been re-evaluated for the later, published version, EASY-2005, and, in most cases, the changes are in the downward direction.

Thirteen nuclides were selected for inclusion in the activation calculations. These were chosen on the basis of importance for dose consequences, derived from previous FISPACT calculations of IFMIF Li loop activation [8].

3. Activation calculations

The data were compiled as outlined in the previous section, enabling TRACT to be configured to model the IFMIF lithium loop, and a calculation was then performed to evaluate, for the instant that IFMIF is halted, the activation resulting from a period of operation of 2.5 years.

Table 1 shows results from the middle of the heat-exchanger (the largest component in the loop), which are very similar to global averages for the system as a whole. The quantities reported for each nuclide are the activities in the deposit, base and coolant. These refer to atoms that have deposited, migrated into the matrix of the wall, or reside in the coolant, respectively. The coolant atoms comprise solubles and crud.

These results show that, for all nuclides, the activity in the base is negligible compared to that in the deposit. Although it is not clear from the table (since surface and volume activity are in different units), it should also be noted that the deposit activity is, in turn, negligible compared to the coolant activity.

Variation in activation along the loop is negligible for all of the coolant nuclides because of their long half-lives compared to the loop transit time (about 80 s) of the Li fluid. The insignificance of surface activity, compared to coolant activity, also applies in the rest of the circuit, indicating that we are able to neglect surface activity when assessing operator dose rates.

The reported results should remain valid for periods of IFMIF operation ranging from about 1–10 years. It is worth noting that, in terms of the overall quantities of individual nuclides present when their levels have reached a plateau, the activation results presented above agree very well with those obtained in an earlier study on IFMIF activation [8].

4. Dose calculations

4.1. Dose rates at shutdown ($t = 0$)

The photon source was evaluated for the activation inventory contained in the coolant only, since surface activation is negligible. This inventory (as given by Table 1) remains constant throughout the loop, as we have noted. It was therefore used in a calculation with FISPACT to obtain the corresponding gamma-spectrum in 24 energy groups. The neutron and photon transport Monte Carlo code, MCNP-4C, was then used with this spectrum, and dose rate conversion factors derived from Ref. [9], to calculate operator dose rate for two different cases relating to the Li loop geometry.

Table 1
Activities at the mid heat-exchanger position of the IFMIF Li loop, at $t = 0$ (shutdown)

Nuclide	Deposit (Bq/m^2)	Base (Bq/m^2)	Coolant (Bq/m^3)
Nb 95	6.78×10^{2}	3.61×10^{-3}	2.68×10^{6}
Mn 56	3.92×10^{4}	3.05×10^{-2}	4.81×10^{8}
Co 58	8.51×10^{4}	7.58×10^{1}	3.17×10^{8}
Mn 54	1.02×10^{5}	3.65×10^{2}	3.02×10^{8}
V 52	2.82×10^{2}	9.86×10^{-8}	9.70×10^{7}
Al 28	3.32×10^{1}	1.43×10^{-8}	2.17×10^{7}
Co 56	5.86×10^{3}	5.73	2.16×10^{7}
Ni 57	5.40×10^{3}	1.42×10^{-2}	2.56×10^{7}
Co 57	6.91×10^{4}	2.99×10^{2}	2.10×10^{8}
Nb 95m	1.26×10^{2}	6.19×10^{-5}	5.53×10^{5}
Mn 52	1.54×10^{3}	6.23×10^{-2}	6.56×10^{6}
Fe 53	7.43×10^{1}	2.47×10^{-6}	1.13×10^{7}
Cr 51	9.20×10^{4}	2.46×10^{1}	3.69×10^{8}
Totals	4.01×10^{5}	7.70×10^{2}	1.87×10^{9}

One case corresponds to exposure from the 20 cm diameter piping which transports the Li between the various loop components. The other corresponds to exposure from the entire Li inventory, assumed, for simplicity, to occupy a spherical volume (radius 1.3 m).

In the case of the 20 cm (inside diameter) piping, a 20 m length with cylindrical geometry (an idealised configuration) and wall thickness of 8.2 mm, was specified for the MCNP calculation, with dose rate being evaluated at the mid-plane, both at the pipe surface (contact dose rate) and at a position 1 m from the surface.

Similarly, for the full inventory, *contact* and 1 m dose rates were also evaluated. For each of these two geometries, results were obtained for two conditions. The first was defined by the assumption that the radioactive source was uniformly distributed throughout the bulk of the Li, and the second by the alternative assumption that the whole of the source was evenly distributed over the bounding surface of the Li. So these conditions can be thought of as corresponding to 'no plating out' and 'all plating out', respectively. The results of these calculations appear in Table 2.

It is evident from Table 2 that, for the pipework, there is no significant difference between the two cases of *all-plating-out* and *no-plating-out*, for either the contact or 1 m dose rates. The reason for this was found to be scattering of the gamma-photons by the 8.2 mm steel pipe wall, changing the directional character of photons emerging from the lithium to a form which is insensitive to any axially-symmetric source redistribution. Hence the omnidirectional (as opposed to planar) flux of photons at any point outside the pipe, and consequential dose rate, are also insensitive to such redistribution.

Table 2
Dose rates for both 20 cm diameter piping (cylindrical geometry) and the full Li inventory (spherical geometry) at $t = 0$ (shutdown)

Source distribution	Contact dose rate (μSv/h)	1 m Dose rate (μSv/h)
20 cm Diameter pipe		
Uniform	147	12.0
Plated out	151	11.2
Full Li inventory (sphere)		
Uniform	1180	220
Plated out	13300	411

The effect of shielding by the SS316 pipe wall is included in the cylindrical case.

In the case of the full Li inventory, on the other hand, no account was taken of any surrounding steel structure. So the source distribution *does* make a difference to dose rate. Contact dose rate is about a factor of 10 higher for *all-plating-out* compared to *no-plating-out*. But there is only around a factor of 2 difference between the two cases for the 1 m dose rate.

It should be noted that the *full-Li-inventory* calculation is unrealistic in the context of normal operation but it is an assumption used in the earlier report [8] to put an upper bound on potential dose rate. The Li can be drained into the dump tank, if necessary, and the Li sphere assumption approximates the conditions which determine the dose rate in this case. If this happens, it is conservative to assume that the dose rate for the *all-plating-out* case applies since, in practice, the structural material of the tank could significantly increase omnidirectional flux (and thereby the dose rate), as in the case of the pipework. The *full-Li-inventory* dose results of this study agree very well with those obtained in the earlier assessment.

4.2. Dose rate as a function of time after shutdown

The results discussed above relate to time, $t = 0$, and are therefore valid during IFMIF operation after a period of at least 1 year of operation, when the system activation has reached a plateau. For some maintenance tasks it may be necessary to halt IFMIF operation, and to assess these circumstances we need to ascertain dose rates as a function of time after shutdown. The good agreement between the current results and those of a previous study [8] establishes the validity of employing the previously calculated time-evolution curves for

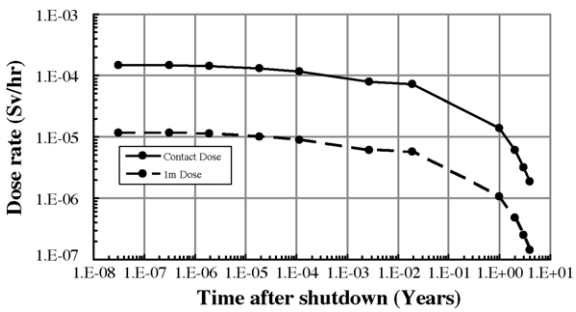

Fig. 1. Contact and 1 m dose rates for 20 cm piping. The data points marked correspond to the following times: 1 and 10 s, 1 and 10 min, 1 h, 1 and 7 days, 1–4 years.

times, $t > 0$. By scaling these curves to fit the current values of piping dose rate, we arrive at the results shown in Fig. 1, which should be valid for times up to 1 year and irradiation periods 1–10 years.

5. Conclusions

The calculations presented above agree very well with the results of an earlier study [8] on overall activation and dose rates. TRACT provides more details than the earlier work but it is very model dependent, and many assumptions need further examination. The present study reveals that the most crucial areas needing further investigation are: (1) solubility, corrosion and dissolution; (2) crud formation; (3) transport modelling of solubles and crud; (4) deuteron activation. Given the requisite data, TRACT is designed to be an appropriate vehicle for exploring the interaction of all of these factors.

Acknowledgements

This work was funded jointly by the United Kingdom Engineering and Physical Sciences Research Council and EURATOM.

References

[1] P.J. Karditsas, Activation product transport using TRACT: ORE estimation of a generic cooling loop under SEAFP-99 conditions, Fusion Eng. Des. 54 (2001) 431–442.
[2] J.-Ch. Sublet, Elemental Compositions of Structural Materials including Impurities and Tramp Elements, SEAFP Report: SEAFP/R-A6/2(93), 1993.
[3] Y. Kato, H. Katsuta, S. Konishi, M. Ogoshi, T. Hua, L. Green, et al., Impurity control in IFMIF lithium loop for IFMIF target facility, J. Nucl. Mater. 258–263 (1998) 394–399.
[4] IFMIF International Team, IFMIF Comprehensive Design Report, January 2004.
[5] O.K. Chopra, P.F. Tortorelli, Compatibility of materials for use in liquid–metal blankets of fusion reactors, J. Nucl. Mater. 122–123 (1984) 1201–1212.
[6] H.U. Borgstedt, C. Guminski, IUPAC Solubility Data Series: vol. 63, Metals in Liquid Alkali Metals, Part I. Be to Os, International Union of Pure and Applied Chemistry, 1996.
[7] R.A. Forrest, EASY-2004 Summary Report, UKAEA Report: UKAEA FUS 505, December 2003.
[8] W.E. Han, N.P. Taylor, Preliminary Investigation of IFMIF Lithium Loop Activation and Associated Operator Dose Rates, IFMIF Report for Task TW4-TTMI-004 of the EFDA Technology Programme, April 2004.
[9] J.F. Breismeister (Ed.), MCNP—A General Monte Carlo Code for Neutron and Photon Transport, Los Alamos Report No. LA-73396-M, Rev. 2, 1986.